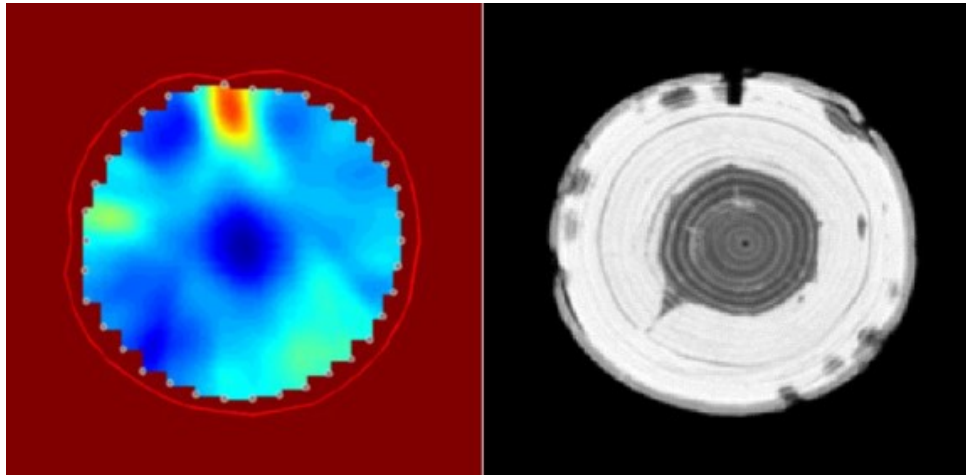# Ultrasound Computed Tomography

Simon Humpohl, II. Physikalisches Institut A, RWTH Aachen

January 25, 2023

Contents

List of Figures

1 Introduction

Ultrasound is a sound wave with a frequency above the limit of human hearing. Unlike electromagnetic waves, sound waves require a medium to propagate (gases, liquids or solids). Ultrasound is therefore not separated from normal sound because of different physical properties, but only because humans cannot hear it. Although this limit varies from person to person, sound frequencies greater than 20 kHz are often referred to as ultrasound. Unlike humans, some animals, such as bats or dolphins, can perceive sound frequencies of up to 200 kHz and use them for orientation (distance measurement by determining the time of flight of a reflected sound pulse). In technology, ultrasound is used to detect objects and measure distances. On the other hand, ultrasound can also be used to manipulate materials (e.g. ultrasonic milling).

An important technical application is imaging procedures with ultrasound (sonography), which are used both in materials testing and in medicine as a diagnostic tool. One imag-ing procedure is the so-called tomography. Tomography (from the ancient Greek "tome", cut, and "graphein", to write), refers to the representation of the internal spatial structures of an object in the form of two-dimensional sectional images. These sectional images are also called tomograms. A tomogram shows the inner structure of an object as it would be after cutting out a thin slice. This is referred to as a non-overlapping representation of the corresponding object layer - in contrast to, for example, the usual X-ray examination or sonography in reflection, in which all structures that lie behind each other in the beam path are superimposed. Tomographic methods are particularly important in medical imaging, but some procedures in the geosciences, physics, palaeontology or material sciences can also be classified under tomographic methods. As an example of application, the cover picture of this instruction manual shows an ultrasound tomography of a tree trunk and an actual cut through the same. Here, ultrasound tomography can be used to investigate e.g. decay or pest infestation on trees in a non-destructive way. Generally speaking, in tomography integrals of a function are determined via straight lines and images are calculated from them by means of inverse radon projection.

2 Physical principles

2.1 Sound waves in a medium

If individual particles are periodically moved out of their rest position in an elastic medium, there is a change in density and pressure that propagates as a continuous elastic wave in the medium due to the coupling with neighboring particles. This pressure wave is called a sound wave. The location- and time-dependent speed of the individual particles around their rest position is called velocity. The propagation speed of the sound wave is called the speed of sound v. It is strongly dependent on the type of sound-conducting medium, its elastic constants and the mutual position of speed and speed of sound.
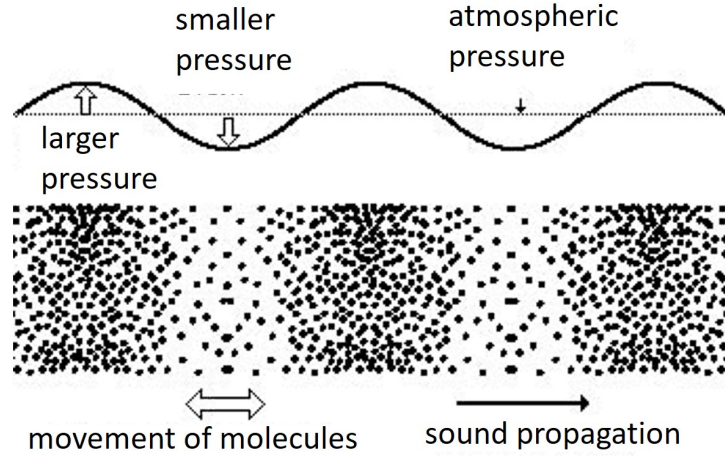
Figure 1: Illustration of a longitudinal sound wave.

If the velocity S is parallel to the direction of propagation of the wave, we speak of longitudinal waves. In the case of transverse waves, the velocity and direction of propagation are perpendicular to each other. Both longitudinal and transverse waves occur in solids, whereas only longitudinal waves occur in gases and liquids. Only longitudinal sound waves are used in this experiment. The wave equation is:

$$\frac{d^2 S}{dt^2} = v^2 \frac{d^2 S}{dx^2} \tag{1}$$

The speed of sound v of longitudinal waves is approximately given by

$$v \approx \sqrt{\frac{E}{\varrho}} \tag{2}$$

with density ϱ and Young's moculus of elasticity E. If the velocity and the density of the medium are known, the so-called wave resistance Z can be calculated:

$$Z = \varrho v \approx \sqrt{\varrho E} \tag{3}$$

If a sound wave hits a boundary layer of two media with different characteristic impedances Z, a part of the sound energy is reflected at the boundary layer. For two media with Z_1 and Z_2, the following applies to the transmission:

$$I_2 = I_1 \frac{4 Z_1 Z_2}{(Z_1 + Z_2)^2} \tag{4}$$

This means that the transmitted sound intensity I_2 decreases with increasing difference in characteristic impedance. Examples of characteristic impedances of different media are shown in Tab. 1: Therefore, it is important for an ultrasonic measurement not to have too large transitions in the characteristic impedance of different media in order to avoid excessive reflections. In particular, transitions to air should be avoided due to the very small characteristic impedance (see Tab. 1). Therefore, the ultrasonic transducers are either placed directly on the object to be examined or the workpiece is under water, like the transducers.

The sound intensity can be reduced not only by reflection at boundary surfaces, but also by sound absorption in the medium. In this case, the absorption coefficient α results from the measured sound amplitude A and the amplitude without measuring sample A_0 according to the attenuation law to (s is the distance the beam travels in the material):

$$A = A_0 e^{-\alpha s} \quad \Leftrightarrow \quad \alpha = -s \cdot \ln \frac{A}{A_0} = s \cdot \ln \frac{A_0}{A} \tag{5}$$

3

Material	ϱ (kg/m^3)	v (m/s)	Z (Ns/m^3)
Air	1.25	343	429
Water	998	1484	$1.481 \cdot 10^6$
Acryl glass	1180	2750	$3.245 \cdot 10^6$
Brass	8553	4430	$3.789 \cdot 10^7$

Table 1: Density, longitudinal sound velocity and characteristic impedance of selected materials at room temperature.

2.2 Generation of ultrasonic waves

The piezoelectric effect is often used to generate ultrasound. Ultrasonic transducers are made of a piezoelectric material, such as SiO_2 (quartz), $BaTiO_3$ and $LiNbO_3$. The material is cut into small, round plates and coated on both sides with silver or gold electrodes. The mechanical deformation of a piezoelectric material leads to a change in the relative distances of positive and negative ions within the atomic lattice, resulting in a voltage drop along a polar axis. Conversely, applying a voltage from the outside leads to a mechanical deformation of the material, which is called the inverse piezoelectric effect. An alternating voltage is used to generate a mechanical oscillation of the piezo. Depending on the crystal orientation and the excitation frequency, the oscillation can be perpendicular or parallel to the surface of the transducer and thus generate either a longitudinal or a transverse ultrasonic wave. Thus, on the one hand, the transducers can be used to induce an ultrasonic wave into the sample and, on the other hand, they can also be used to detect the sound wave. To increase the amplitude of the mechanical vibration, the excitation frequency is set close to the resonance frequency of the transducer. The resonant frequency is determined by the thickness and density of the transducer material. In our experiment, ultrasonic transducers with resonant frequencies of 1 MHz, 2 MHz and 4 MHz are used, which can be used both as transmitters and receivers and emit longitudinal ultrasonic waves. To increase the mechanical coupling, an ultrasound gel is placed between the transducer and the sample surface, which has a wave resistance similar to that of water and thus reduces reflections at the interface with the sample.

## 3 Ultrasonic measurement methods

3.1 Ultrasound A-Scan (Reflection measurement)

The A-scan procedure was at the beginning of ultrasound diagnostics. Here, an ultrasound wave packet (sound pulse) is emitted periodically. With each sound pulse, a time line is written on the screen (x axis), which can be displayed as the path of the sound pulse if the speed of sound is known. Between the sound pulses, the echoes reflected from the boundary surfaces are received and displayed as amplitude peaks (y axis). This method was first used in shipping as an echo sounder in about 1912 and was used for non-destructive material testing in the 1930s. In 1949, it was introduced into medicine by G. Ludwig (Pennsylvania) and became very important in echoencephalography under the name "A-scan", which was still being carried out into the 1980s. In the course of development, this type of signal processing was replaced by the B-scan procedure due to the lack of anatomical orientation possibilities.

In the "GSView" software, the A-scan can be started by pressing a correspondingly marked button. A diagram of the reflected sound amplitude is plotted against the time of flight. It should be noted that a large intensity is always displayed for times close to zero, as part of the ultrasonic pulse is reflected back directly from the transducer/sample interface.
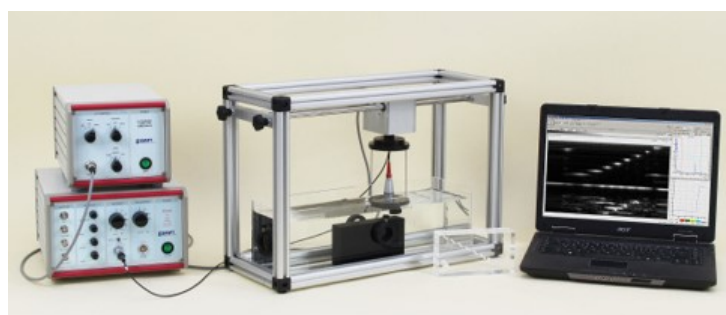
3.2 Ultrasonic measurement in transmission

In this part of the experiment, the speed of sound and the absorption of various materials are to be measured using a sound pulse measurement in transmission. For this purpose, a transmitter and a receiver transducer are coupled to the sample (with ultrasound gel). The speed of sound can be calculated from the temporal distance between the transmitter pulse and the receiver pulse. The amplitude of the envelopes of the sound pulses provides information about the attenuation value. Acrylic rods with different lengths are available. This measurement is to be carried out for different ultrasonic frequencies (1 MHz, 2 MHz, 4 MHz).
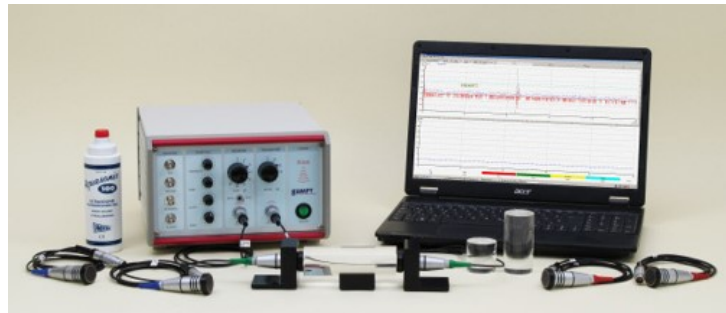
Figure 2: Experimental setup for determining the speed of sound and sound absorption using transmission measurements.

3.3 Ultrasound B-Scan (2D, reflection)

The name B-scan comes from the English "brightness scan" and represents a two-dimensional mapping of the reflected amplitude values in grey levels. To obtain a B-scan, the ultrasound transducer must therefore be moved along a line at constant speed, while the reflection signals are recorded as grey values over the time of flight. Today, so-called array scanners are used for this purpose in medicine, in which several ultrasound transducers are arranged on a line and are controlled and read out one after the other. This eliminates the need to constantly move the ultrasound transducer. To perform a B-scan, the transducer is attached to the stepper motor with the corresponding holder. Make sure that the transducer is slightly immersed in the water. The measurement object is completely submerged under the water. Now, with the help of the step-per motor control, the transducer can be moved over the sample at a constant speed and the reflected signal can be recorded. Here, the positions of defects in a black test block are to be measured.

Figure 3: Experimental setup for measuring a sample using the B-scan method.

3.4 Ultrasound computer tomography (2D, transmission)

In general, a computer tomography (CT for short) is an imaging measurement procedure for the non-reactive acquisition of locally distributed measured quantities. The aim is to image a physical quantity

(in this experiment, e.g. the absorption coefficient or the speed of sound) as a function of location (x,y) in a cross-sectional plane of the object to be examined in order to gain information about further properties. The best-known examples are X-ray and ultrasound procedures in medicine. While most medical ultrasound procedures evaluate the reflected signals (B-scan), X-ray tomography and ultrasound tomography measure the intensity of the transmitted waves and determine the attenuation (absorption) from this. In this experiment, in addition to this absorption tomogram, a sound velocity tomogram is also recorded, which represents the speed of sound at each location (x,y) of the sample.

3.4.1   Determination of the absorption tomogram

In the following, the procedure for creating CT images is first explained on the basis of ultrasound absorption. If an ultrasound pulse is sent through a cross-section of the body to be examined, the sound intensity is attenuated, depending on the absorption coefficient. The absorption coefficient is generally not spatially constant, but a function of the location vector $\vec{x}$. For example, ultrasound tomography in breast diagnosis takes advantage of the fact that breast tissue and tumor tissue absorb sound to different degrees. For location-dependent absorption coefficients, the damping law

$$A = A_0 e^{-\alpha s} \tag{6}$$

applies no longer, and is described by the more general Lambert-Beer damping law, whereby the absorption coefficient can now depend on the location $\vec{x}$:

$$A = A_0 \exp\left(-\int_S^E \alpha(\vec{x})\,ds\right) \tag{7}$$

The attenuation of the sound intensity on the way from the transmitter S to the receiver E is thus described by the line integral along the distance s from S to E via the local distribution of the attenuation coefficient. A transformation results in:

$$\ln\left(\frac{A}{A_0}\right) = -\int_S^E \alpha(\vec{x})\,ds \tag{8}$$

where $\ln\left(\frac{A_0}{A}\right)$ represents a projection $P(x,y)$ of α in the coordinates x,y:

$$P(x,y) = \ln\left(\frac{A_0}{A}\right) = \int_S^E \alpha(\vec{x})\,ds \tag{9}$$

The name projection comes from the fact that $P(x,y)$ consists of the projected values of $\alpha(\vec{x})$ integrated in the s-direction. To obtain a good tomographic image, however, a single measurement is not sufficient. More information is obtained by looking at the projection along many different rays through the object. To do this, for example, one moves the object to be examined through the measuring beam and also lets it rotate, as shown in Figure 4.

Each individual measurement is thus defined by the angle of rotation θ, which determines the direction of the sound beam, and by the lateral coordinate l, the displacement path of the object under examination (Fig. 5). If one considers all measurements taken at a fixed angle θ, one obtains a projection $P(l,\theta)$. For the sake of completeness, it should be mentioned that in X-ray tomography an entire field of detectors is exposed to a fanned-out X-ray beam. Here, the transmitter and detector field rotate around the object to be examined. The quality of the tomography image increases with the number of projections taken during the rotation.

It now makes sense to convert the coordinates x,y into the known quantities l (travel distance) and θ (angle of rotation). The following applies to a point $\vec{s}$ of the sound beam and $\vec{l}$ of the travel distance:

$$\vec{s} = s \begin{pmatrix} \sin\theta \\ \cos\theta \end{pmatrix} \quad ; \quad \vec{l} = l \begin{pmatrix} \cos\theta \\ \sin\theta \end{pmatrix} \tag{10}$$
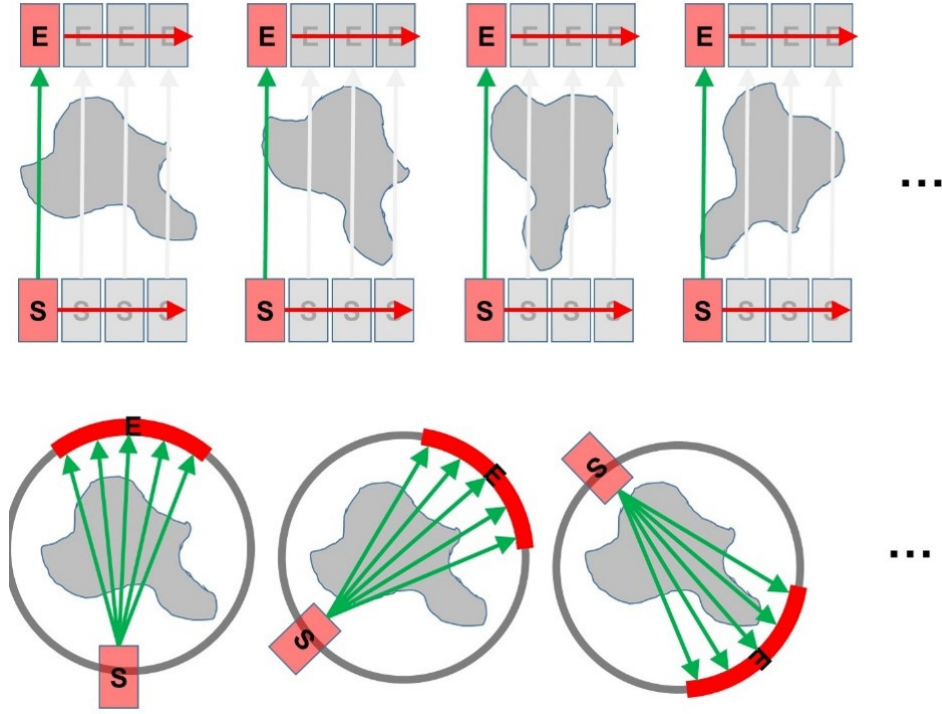
Figure 4: Comparison of ultrasound CT (top) and X-ray CT (bottom). In ultrasound CT, either the object is moved linearly through the ultrasound beam (as in our experiment) or transmitters or receivers are moved linearly, or there is a linear field of transmitters and receivers. After this linear scan, the object is rotated and another scan is per-formed. In X-ray CT, only one transmitter (X-ray tube) and one receiver array are used. The aperture angle of the X-ray beam is chosen so that the array is completely illuminated. Likewise, after a scan, the transmitter / receiver is rotated around the object.

For the object point follows:

$$\vec{x} = \vec{l} + \vec{s} = \begin{pmatrix} l \cdot \cos\theta - s \cdot \sin\theta \\ l \cdot \sin\theta + s \cdot \cos\theta \end{pmatrix} \tag{11}$$

and thus for the projection:

$$P(l,\theta) = \int_S^E \alpha \begin{pmatrix} l \cdot \cos\theta - s \cdot \sin\theta \\ l \cdot \sin\theta + s \cdot \cos\theta \end{pmatrix} ds \tag{12}$$

This conversion is also commonly referred to as the Radon transformation. It is a two-dimensional integral transformation, since the functions $P(l,\theta)$ and $\alpha(x,y)$ each depend on two variables. The name Radon transformation comes from its inventor, the mathematician Johann Radon, who also specified the associated inverse transformation in 1917. But it was not until the 1960s that the Radon transform gained practical significance through the development of X-ray computed tomography.

The measured values $P(l,\theta)$ represent a function of the variables l and θ, which emerges from the function $\alpha(x,y)$ which also depends on two variables. One will therefore expect that $P(l,\theta)$ and $\alpha(x,y)$ contain the same amount of information and that one can calculate the sought distribution (x,y) from the $P(l,\theta)$ known from the measurements. From the above description of the measurement process, the characteristic features of a tomographic measurement procedure are already expressed:

- The measurement is carried out without interfering with the object being measured, as the transmitter and receiver are located outside the object. This makes the tomographic methods non-destructive. The energy of the measuring beam used must of course be low enough not to damage the object being measured.

7
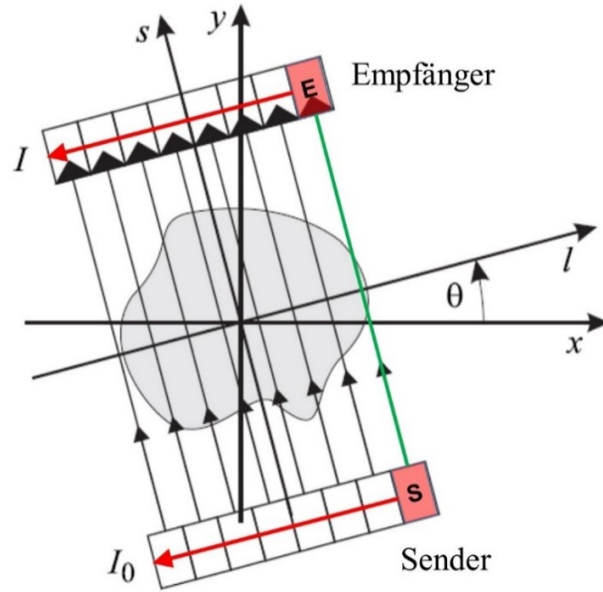
Figure 5: To obtain a complete tomogram, the sound beam is passed through the object (or the object through the beam) and rotated.

- A single measurement provides an integral average over the quantity of interest in the form of a line integral.

- In order to obtain the local distribution of the quantity of interest, a very large number of individual measurements along different rays through the measurement object are necessary.

These three properties concern the measurement data acquisition. The procedure of how to process the projections $P(l,\theta)$ to obtain the distribution $\alpha(\vec{x})$ from them is essentially an inversion of the Radon transform, also called the filtered back-projection.

3.4.2 The filtered back-projection

The filtered back-projection reconstructs an original 2D image from a set of one-dimensional projections from different directions. For this purpose, the projections are first filtered and then back-projected over the image surface in the respective direction. The method has the advantage that it requires little computing power and is therefore very fast.

When processing the measured values to reconstruct $\alpha(\vec{x})$, note that only finitely many measured values $P(l_i,\theta_i)$ ($i = 1...N$, $j = 1...M$) are known. Nevertheless, let us first assume that the projections $P(l,\theta)$ are known for all values of l and θ ($0 \leq \theta < \pi$) and only then consider the digital realization.

Since the filtering is carried out with the help of a Fourier filter, the Fourier transformation should first be briefly discussed again. This is generally defined for a function $f(l)$ by:

$$F(k) = \int_{-\infty}^{+\infty} f(l)e^{-ikl}\, dl \tag{13}$$

The Fourier transform $F(k)$ belonging to $f(l)$ is also called spectrum of $f(l)$ and is a function of the real variable k, which has the dimension 1/m and is called spatial frequency variable. From the spectrum one arrives at the original function $f(l)$ with the inverse Fourier transform:

$$f(l) = \frac{1}{2\pi} \int_{-\infty}^{+\infty} F(k)e^{ikl}\, dk \tag{14}$$
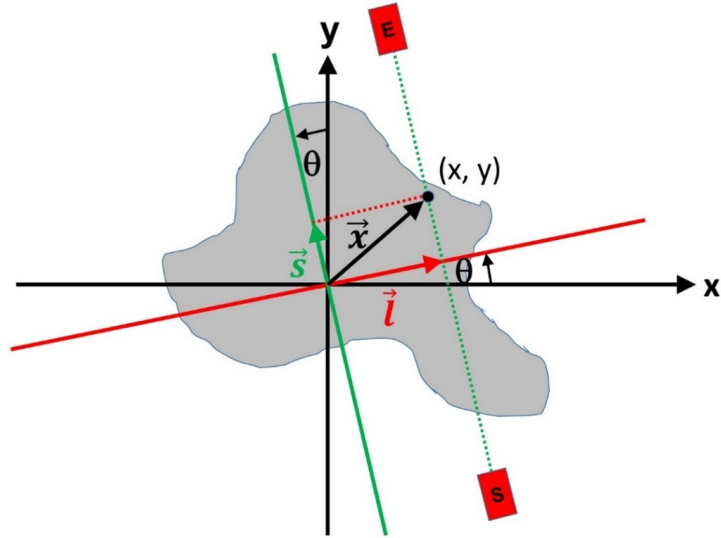
Figure 6: Description of the object point $\vec{x} = (x,y)$ with the help of the angle of rotation θ, as well as the distances l (linear traverse) and s (sound beam path).

The Fourier transform of a projection is linked via the projection-slice theorem to a section through the Fourier transforms of the original function. This can be understood graphically by the fact that the projection along an axis is equivalent to the Fourier integral with $k_s = 0$, i.e. $e^{ik_s s} = 1$:

$$F\left(P(k,\theta)\right) = \int_{-\infty}^{+\infty} \int_S^E \alpha \begin{pmatrix} l \cdot \cos\theta - s \cdot \sin\theta \\ l \cdot \sin\theta + s \cdot \cos\theta \end{pmatrix} ds\, e^{-ikl}\, dl \tag{15}$$

$$= \left[\int_{-\infty}^{+\infty} \int_S^E \alpha \begin{pmatrix} l \cdot \cos\theta - s \cdot \sin\theta \\ l \cdot \sin\theta + s \cdot \cos\theta \end{pmatrix} e^{-i(kl + k_s s)}\, ds\, dl \right]_{k_s = 0} \tag{16}$$

$$= F_2\alpha(k,\theta) \tag{17}$$

Here, $F\left(P(k,\theta)\right)$ stands for the Fourier transform of the projection $P(l,\theta)$ belonging to a fixed angle θ, and $F_2\alpha(k,\theta)$ for a cut along this angle through the origin of the two-dimensional Fourier transform of the original function. α can thus be calculated via the inverse Fourier transform in polar coordinates.

$$\alpha\left(\vec{x}\right) = F_2^{-1}FP = \frac{1}{4\pi^2} \int_0^{2\pi} \left(\int_0^\infty kFP(k,\theta)e^{ik(x\cos\theta + y\sin\theta)}\, dk \right) d\theta \tag{18}$$

Since $FP(k,\theta) = FP(-k,\theta+\pi)$, we can change the integral limits and replace k by $|k|$. The inverse Fourier transform in polar coordinates is thus reformulated as a one-dimensional Fourier transform filtered with a ramp filter (Ram-Lak filter) $|k|$ followed by a back-projection and thus represents the filtered back-projection for all possible angles θ between 0 and π:

$$\alpha\left(\vec{x}\right) = \frac{1}{2\pi} \int_0^\pi \left(\frac{1}{2\pi} \int_{-\infty}^{+\infty} |k|FP(k,\theta)e^{ik(x\cos\theta + y\sin\theta)}\, dk \right) d\theta \tag{19}$$

For a thorough derivation, please refer to references [1, 2].

Figure 7 again illustrates the facts of projection and back-projection. As an object, we take a circular screen that is illuminated from the side with a lamp (transmitter). The shadow cast on the opposite screen (receiver) is a line with a length equal to the diameter of the original disc. The back-projection (unfiltered in this case) is a smearing of the line back across the entire image plane. This results in a stripe across the image plane with a width again equal to the diameter of the disc. If one performs another projection at $90°$ to the first and a corresponding back-projection, one obtains a square in the center of the image with edge lengths that correspond to the diameter of the original
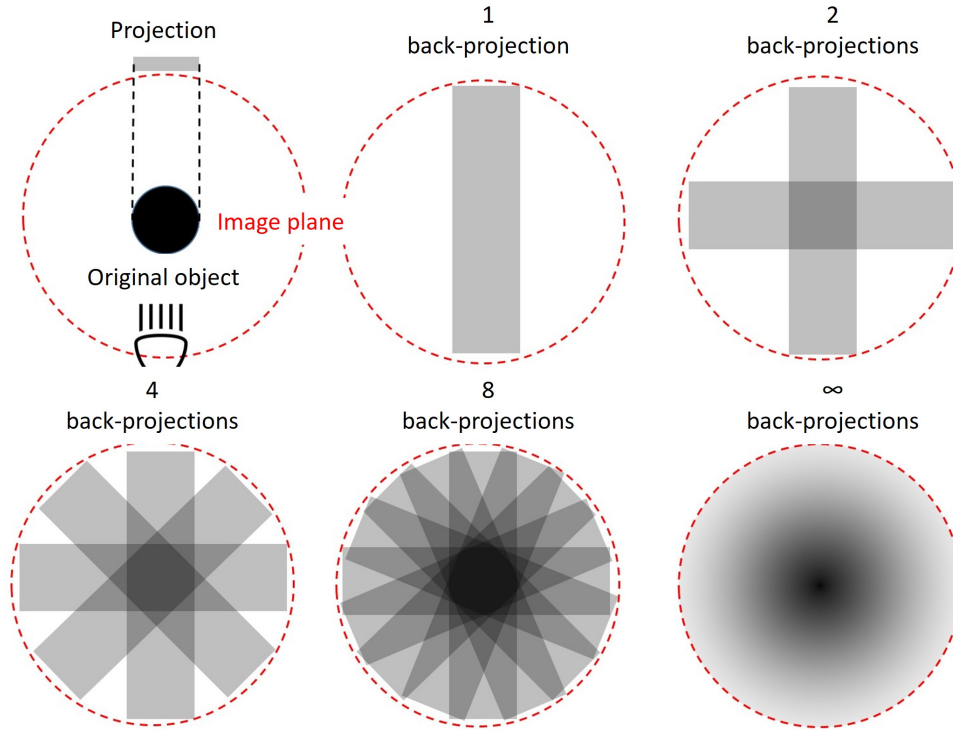
Figure 7: Illustration of projection and back-projection: The original object (circular disc top left) is projected sideways onto a screen using a lamp. The backprojection "smears" the shadow cast back across the image plane, creating a stripe. The more projections / backprojections from different directions are added, the better the circular disc is reproduced, but with blurred edges.

object. The more projections and back-projections are carried out at different angles, the better the original circular disc is reproduced. However, the edge of the disk is not sharply reproduced in the add-ed/integrated back-projections because the shadows of the projections still overlap out-side the center. In Fourier space (k-space), this means that high frequencies (k-values), such as those occurring at sharp edges, are underrepresented in the image. Therefore, Fourier filtering is performed with a high-pass filter, which is described as a filtered back-projection. As shown above, a ramp filter (Ram-Lak filter) ensures that sharp object contours are reproduced correctly.

In the following, the individual operations from the above equation are explained again in detail. First, the following steps are carried out for a fixed angle θ, at which a projection was taken:

1. Fourier transformation of the projection $P(l,\theta)$, i.e. calculation of $P(k,\theta)$

$$FP(k,\theta) = \frac{1}{2\pi} \int_{-\infty}^{+\infty} P(l,\theta) e^{-ikl} \, dl \qquad (20)$$

2. Multiplication of $FP(k,\theta)$ with filter function $|k|$. This high-pass filter is called a Ram-Lak filter (after the inventors of the filter Ramachandran and Lakshminarayanan) or ramp filter and is abbreviated FP_{F}:

$$FP_{\mathrm{F}}(k,\theta) = |k|FP(k,\theta) \qquad (21)$$

3. The integral in the parenthesis is an inverse Fourier transform applied to $FP(k,\theta)$ and therefore yields the original function belonging to $FP(k,\theta)$:

$$P_{\mathrm{F}}(l,\theta) = \frac{1}{2\pi} \int_{-\infty}^{+\infty} |k|FP(k,\theta)e^{ikl} \, dk \qquad (22)$$

This third step thus consists of an inverse Fourier transformation. The result $P_{\mathrm{F}}(l,\theta)$ is called a filtered projection because it emerges from the projection $P(l,\theta)$ by filtering with $|k|$.

4. Now the substitution of the variables

$$\vec{x} = \begin{pmatrix} x \\ y \end{pmatrix} = \begin{pmatrix} l\cos\theta - s\sin\theta \\ l\sin\theta + s\cos\theta \end{pmatrix} \tag{23}$$

carried out in the 3$^{\text{rd}}$ step is reversed, i.e. one must now express l with the help of x and y again. This is done by projecting the location vector onto the l-axis:

$$l = \vec{x} \cdot \hat{e}_l = \begin{pmatrix} x \\ y \end{pmatrix} \cdot \begin{pmatrix} \cos\theta \\ \sin\theta \end{pmatrix} = x\cos\theta + y\sin\theta \tag{24}$$

where $\hat{e}_l$ represents the unit vector in l direction. That is, the value of the filtered projection P_{F} at location l is assigned to all those pixels $\vec{x}$ that satisfy the equation $l = x\cos\theta + y\sin\theta$. In other words, the filtered projection $P_{\text{F}}(l,\theta)$ is "smeared" along the ultrasonic beam direction s at constant l. This process corresponds to the inverse of the projection where up-integration was performed along the same straight line and is therefore referred to as back-projection. Thus the filtered back-projection is now:

$$P_{\text{F}}(l,\theta) = P_{\text{F}}\left((x\cos\theta + y\sin\theta),\theta\right) \tag{25}$$

5. After these four steps have been carried out for all θ, integration via θ must finally be carried out. In practice, however, one always has only a finite number of projections available, whereby the individual angles θ_i $(i = 1,2,...N)$ are equidistant here: $\theta_i = \frac{1}{N}\pi$. The integration via $d\theta$ can therefore be replaced by a summation with discrete angles of $\Delta\theta = \frac{\pi}{N}$:

$$\alpha\left(\vec{x}\right) = \frac{1}{2\pi} \sum_{i=1}^{N} P_{\text{F}}\left((x\cos\theta_i + y\sin\theta_i),\theta_i\right) \cdot \frac{\pi}{N} \tag{26}$$

Overall, one can expect good reconstruction results, provided that the number of projections is not too small. This is the case in medical X-ray tomography with $N \approx 100$ projections, each consisting of ≈ 100 individual measurements. In this practical experiment, the number of measured angles is to be varied and the connection with the imaging accuracy discussed. Measurement objects for which the function $\alpha(\vec{x})$, does not change too much locally can be measured with fewer projections and the measurement data can be interpolated.

3.4.3 Filtering problems

Comparing the filtered with the unfiltered back-projection, one can see that the Fourier filtering with the Ram-Lak filter provides a much better reproduction of the object outlines (see Fig. 8).
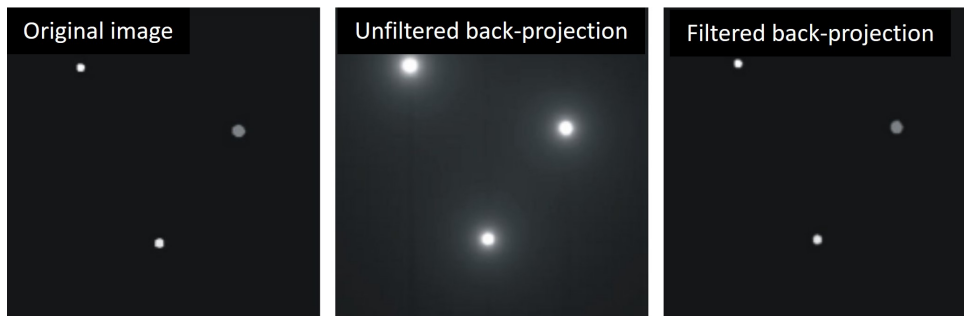

Figure 8: Comparison of unfiltered and filtered back-projection (with Ram-Lak filter) to the orig-inal image. The Ram-Lak filtering clearly reproduces the edges of the objects better [3].

A disadvantage of Ram-Lak filtering, however, is the increased imaging of high-frequency noise (e.g. due to electrical noise of the detectors). A possible improvement is obtained by slightly weakening the high-pass filtering at higher frequencies. This can be done by multiplying the Ram-Lak filter $F(k) = |k|$ with another low-pass filter. The software "GSView" displays the unfiltered back-projection as well as the filtered back-projection with the Ram-Lak filter attenuated towards high frequencies by an additional Shepp-Logan filter. The mathematical equation of a Shepp-Logan low-pass filter is:

$$F(k) = \frac{\sin \frac{\pi k}{2C}}{\frac{\pi k}{2C}} \tag{27}$$

where C is the so-called cut-off parameter and may lie between 0 and 1. C is already fixed in the display software "GSView" and cannot be changed here. A graphical illustration of the filters is shown in Figure 9. You can see the Ram-Lak filter (high-pass) necessary for the filtered back-projection, as well as the Shepp-Logan low-pass filter and the multiplication of both, which results in an attenuation of the linear increase of the Ram-Lak filter trans-mission at high |k| values.
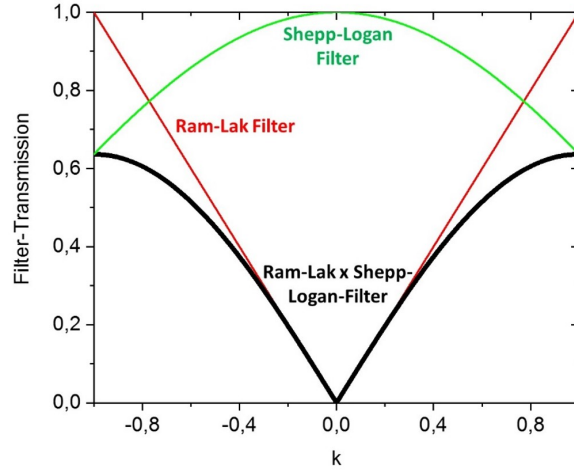
Figure 9: Graphical representation of the filter functions for the back-projection. The multiplication of Ram-Lak filter with the Shepp-Logan filter suppresses high-frequency noise of the detectors better.

3.4.4 Determination of the velocity tomogram

For the determination of the sound velocity v at each object point $\vec{x}$ one proceeds analogously to the absorption determination. The measuring apparatus determines the transit time t along the beam path s of an ultrasonic pulse through the sample:

$$t = \int_S^E \frac{1}{v(\vec{x})} \, ds \tag{28}$$

Thus, in this case, the projection is given by:

$$P(l,\theta) = t = \int_S^E \frac{1}{v(\vec{x})} \, ds = \int_S^E \frac{1}{v\left(\begin{pmatrix} l\cos\theta - s\sin\theta \\ l\sin\theta + s\cos\theta \end{pmatrix}\right)} \, ds \tag{29}$$

All further steps are carried out as described above to obtain $v(\vec{x})$:

$$\frac{1}{v(\vec{x})} = \frac{1}{2\pi} \sum_{i=1}^{N} P_F\left((x\cos\theta_i + y\sin\theta_i),\theta_i\right) \cdot \frac{\pi}{N} \tag{30}$$

12

3.4.5 Experimental set-up of computed tomography

The experimental setup for computed tomography essentially consists of a water basin with connections for the ultrasound transducers, an aluminum profile frame for the stepper motor mount, as well as the control units for the ultrasound pulse generation and the stepper motor control (see Fig. 10). The CT sample is magnetically attached to the sample plate (on the stepper motor) and the sample is positioned exactly in the middle between the two ultrasound transducers with the help of the stepper motor control. Then the sample plate is moved by half the scan path (l) so that the sample is completely outside the sound beam at the edge. This is important so that the time t_0 (travel time in water) can be determined.
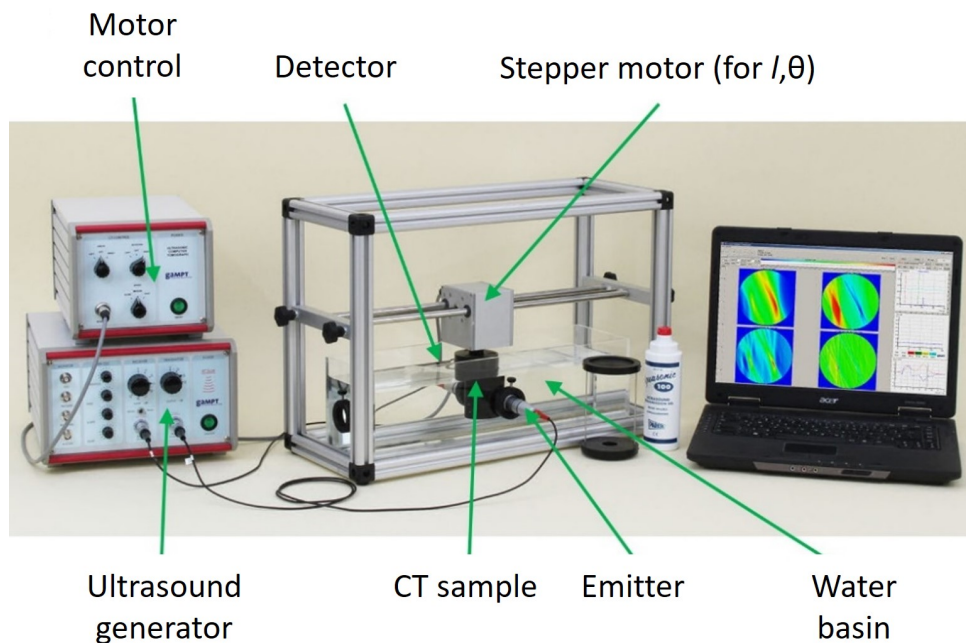
Figure 10: Experimental set-up for measuring a sample using ultrasound computed tomography.

After setting the scanning accuracy (distance of the measuring points along l) and the number of angular intervals, the CT scan is started. During the measurement, the individual line scans are observed and the formation of the tomograms for v and α is followed by superimposing the projections of the line scans. Further details on the measurement can be found in the GAMPT operating instructions.

4 Info on CT measurement recording

The speed of sound is determined by the measured transit time of the ultrasonic pulse. The starting point is the transmission of the pulse by the transmitter. The transit time is saved when the set "threshold" value of the amplitude is reached. Care must be taken to find a suitable value for the threshold. If the threshold value is too small, the speed measurement can already be triggered by noise in the signal. If it is too large, no speed can be measured at all if the signal attenuation is too high. It is therefore important to first try out suitable values for the threshold value, the transmitting power ("output") and amplification ("gain"). At high gain values, electronic crosstalk of the stepper motor to the measurement signal can be observed. Since the frequency of the crosstalk is different from that of the ultrasonic signal, this **interference can be eliminated by using the Fourier filter**, thus reducing the threshold value.

In addition to simple image files of the diagrams, the GS-Echoview software can also save original data of the individual projections as relative measured values in a file for the amplitude (*_amp.dat), as well as in one for the speed (*_vel.dat) depending on the angle θ and the travel distance l. The data is saved in an ascii file. The data is saved in an ascii table if "save results to ascii" has been activated. **For the data output, select "none" for "original data"**, otherwise each line scan will be saved additionally and the measurement will become very slow. The software saves the values for the sound amplitudes in:

$$\ln \frac{A_0}{A} = \ln \frac{1\,\text{V}}{A} \tag{31}$$

The amplitude is measured by the signal of the receiver piezo in V and here still normalized to $A_0 = 1\,\text{V}$. For the speed, values of

$$\frac{v_0 - v}{v} \cdot 100 = \left(\frac{v_0}{v} - 1\right) \cdot 100 = \left(\frac{t_0}{t} - 1\right) \cdot 100$$

are stored. The velocity ratio is given by the running time ratio. For this purpose, the time t_0 is automatically determined outside the sample before each tomography measurement (travel time in water). Therefore, it must be noted that the **travel distance of the sample is chosen so large that the ultrasonic beam no longer passes through the sample at the beginning of the measurement**.

Under the link[1] you will find the file "file_reader.py" which contains functions for reading the files generated by GS-EchoView in python.

5 Tasks

The experimental procedure should be carried out in the following order. Items shown in green are to be done at home:

1. **A-scan** of acrylic glass: Determine the speed of sound and the damping of acrylic glass with the help of an A-scan in transmission. Use 3 rods of different lengths and different ultrasound frequencies (1 MHz, 2 MHz, 4 MHz). Plot the determined transit times against the path length and determine the speed of sound in acrylic glass as accurately as possible. Is the speed of sound dependent on frequency? Discuss possible sources of error. Can you say anything about the transit times in the ultrasonic sensor itself? Determine the frequency-dependent damping of the ultrasonic wave.

2. **B-scan** of the the black acrylic block: Using the scanner, perform a B-scan of the black acrylic block at an ultrasound frequency of 1 MHz, 2 MHz and 4 MHz from the top as well as the bottom side. Create a map with the positions of the disturbances (with error bars) in the acrylic glass. What can be said about the resolution in the direction of the sound beam at different frequencies? What can be said about the lateral resolution (perpendicular to the sound beam). What image artefacts can be seen? Where do these come from?

3. **CT-Scan** on the CT sample: optimize the parameters for 1 MHz, 2 MHz and 4 MHz transducers:

   (a) Determine the transit time of the sound pulse through the water basin. Use this information to set the "interesting time range" for the CT measurement in the measurement diagram.

   (b) Determine the threshold value for starting and stopping the time-of-flight measurement (important for velocity measurement).

---

[1] https://git.rwth-aachen.de/physik_praktikum/ultraschall_versuch/raw/master/file_reader.py?
inline=false

(c) Optimise the values for output amplitude ("output") and receiver gain ("gain") and filter out disturbances that occur at high gain values by the stepper motor with the help of the Fourier filter. **The values can be different for the absorption CT and the velocity CT!**

(d) Perform CT scans for absorption at $1\,\mathrm{MHz}$, $2\,\mathrm{MHz}$ and $4\,\mathrm{MHz}$ with different numbers of angles ($5°$ or less).

(e) Plot the added (unfiltered) absorption back-projections as well as the speed of sound using Python (submit code with the script).

(f) Calculate a CT image from the addition of the filtered back-projections (with Ram-Lak filter) and plot the spatially resolved absorption coefficient using a Python algorithm (submit code with the script) and the correct scales. What is the difference between CT images obtained from unfiltered and filtered back-projection? If pack-ages like scikit-image are used, please indicate where (file and line) in these the relevant steps, i.e. Fourier transform and filtering are performed.

(g) Plot the absorption CT image for 3 different numbers of back-projections and discuss the spatial resolution.

(h) Discuss any measurement artefacts or spatial resolution as a function of ultra-sound frequency.

6 Further reading

- M. Seiraffi, A. Trächtler, B. Menz, D. Schupp: Ultraschall-Computertomographie, Universität Karlsruhe

- Filtered back-projection (Gefilterte Rückprojektion),
  https://de.wikipedia.org/wiki/Gefilterte_R%C3%BCckprojektion

- M. Schickert, F. Bonitz, A. Ulanov, B. Müller: Materialcharakterisierung mit Ultraschall- und Radar-Tomographie – Fäuleerkennung in Holzstämmen, Materialforschungs- und -prüfanstalt (MFPA), Bauhaus-Universität Weimar

- http://www.ultraschallmuseum.de/download/Tafeln-7-11Korr-Febr2007-Internet.pdf

- http://www.laermorama.ch/m1_akustik/schall_w.html

References

[1] C. L. Epstein, ed., "Introduction to the mathematics of medical imaging," (Society for Industrial and Applied Mathematics, 2007) Chap. 6.

[2] A. C. Kak and M. Slaney, "Principles of computerized tomographic imaging," (Society for Industrial and Applied Mathematics, 2001) Chap. 3.

[3] M. Boin, "Kompensation von artefakten bei der rekonstruktion tomographischer datensätze," (2005), diploma thesis, FHW Berlin (2005).